Available online at www.sciencedirect.com
ScienceDirect
Tetrahedron
Tetrahedron 63 (2007) 5236–5243

Investigation of the barrier to the rotation of carbamate and amide C–N bonds in antidepressant (6a*R**,11b*S**)-7-[carbobenzyloxy-L-alanyl]-2-[(4-methylphenyl)sulfonyl]-1,2,3,4,6,6a,7,11b,2,12a(*S*)-decahydropyrazino[2′,1′:6,1]pyrido[3,4-*b*]indole by dynamic NMR and molecular mechanics☆

Aparna Anand,[a] Abhijeet Deb Roy,[a] Ruchika Chakrabarty,[b] Anil K. Saxena[b,*] and Raja Roy[a,*]

[a]*Division of SAIF, Central Drug Research Institute, Lucknow 226 001, UP, India*
[b]*Medicinal and Process Chemistry Division, Central Drug Research Institute, Lucknow 226 001, UP, India*

Received 1 December 2006; revised 14 March 2007; accepted 29 March 2007
Available online 4 April 2007

Abstract—Two concurrent exchanges arising due to the restricted rotation around the carbamate C–N bond and amide C–N bond were observed in (6a*R**,11b*S**)-7-[carbobenzyloxy-L-alanyl]-2-[(4-methylphenyl)sulfonyl]-1,2,3,4,6,6a,7,11b,2,12a(*S*)-decahydropyrazino-[2′,1′:6,1]pyrido[3,4-*b*]indole by NMR spectroscopic experiments. A total of four low energy conformers were evaluated in the molecule, out of those, two were observed because of the restricted rotation of the amide C–N bond in $CDCl_3$ and two were observed due to restricted carbamate C–N bond rotation in DMSO-d_6 and $(CD_3)_2CO$. The barrier to the rotation ($\Delta G^{\ddagger}$) around carbamate C–N bond and amide C–N bond was determined using dynamic NMR calculations. Molecular mechanics calculations also provided evidence for the presence of four low energy conformers for the compound due to restricted amide rotation and carbamate C–N bond rotation, with the value of barriers ($\Delta G^{\ddagger}$) between them of the order of 15.0 kcal/mol, which is in agreement with the dynamic NMR results. Since the molecule has shown potent antidepressant activity, it is proposed that these dynamic properties could influence the activity profile of these classes of molecules.

1. Introduction

In recent years, the kinetics and thermodynamics of the stereodynamic processes occurring due to restricted intramolecular rotation have been extensively explored using dynamic NMR studies.[1] The phenomenon of hindered rotation about carbamate[2] and amide[3] C–N bonds has received much attention as rotational changes play significant role in conformational stereochemistry of a compound, which could influence the activity profile. From the previously reported experimental data, it has been observed that carbamate C–N bond and amide C–N bond have nearly equal barriers to the rotation ($\Delta G^{\ddagger}$).[4] Previously Lectka and Cox demonstrated[4] the effect of various solvents on $\Delta G^{\ddagger}$ of the carbamate and amide C–N bonds, where the rotational barrier of the carbamate C–N bond was found to have least sensitivity toward the solvent polarity. Contrary to that of carbamates, $\Delta G^{\ddagger}$ of the amide C–N bond was considerably increased upon changing the polarity of solvents.[4] Moreover, the lowering of the rotational barrier of carbamate C–N bond has also been reported,[5] which was attributed to the resonance effect exerted by an *N*-substituted aryl ring. This evidence indicated that the barrier to rotation of the carbamate and amide C–N bonds might depend upon some of the other analogous factors, which still remained unexplored. Although much of the work carried out so far specifically deals with the study of solvent effects on $\Delta G^{\ddagger}$ of a molecule containing either the carbamate functionality or amide functionality, there has been no report in the literature regarding the effect on $\Delta G^{\ddagger}$ of either of the functional groups when both of them existed in the same system.

In our ongoing process of synthesizing derivative of CNS active nucleus decahydropyrazino[2′,1′:6,1]pyrido[3,4-*b*]-indole, we synthesized a potential antidepressant molecule (6a*R**,11b*S**)-7-[carbobenzyloxy-L-alanyl]-2-[(4-methylphenyl)sulfonyl]-1,2,3,4,6,6a,7,11b,12,12a(*S*)-decahydropyrazino[2′,1′:6,1]pyrido[3,4-*b*]indole (**4**). During the process of characterization of this molecule the ^{1}H NMR spectrum

☆ CDRI Communication No. 6970.
Keywords: Dynamic NMR; Carbamate; Rotational barrier; Decahydropyrazino[2′,1′:6,1]pyrido[3,4-*b*]indole.
* Corresponding authors. E-mail addresses: anilsak@hotmail.com; rajaroy_cdri@yahoo.com

0040–4020/$ - see front matter © 2007 Elsevier Ltd. All rights reserved.
doi:10.1016/j.tet.2007.03.171

revealed few broad resonances at room temperature, indicating the effect of barrier to the rotation of the carbamate and or amide C–N bond, which led us to the current study. In the present communication, we herein describe the investigation of the barrier to the rotation of carbamate and amide C–N bonds when both are present in a single system. Further calculations of the activation parameters involved in this dynamic exchange process were also determined in two different solvents by two-dimensional exchange spectroscopy and molecular mechanics.

2. Results and discussion

2.1. Synthesis

We synthesized a new analogue of CNS active drug centbutindole,[6] (6a*R**,11b*S**)-7-[carbobenzyloxy-L-alanyl]-2-[(4-methylphenyl)sulfonyl]-1,2,3,4,6,6a,7,11b,12,12a(*S*)-decahydropyrazino[2′,1′:6,1]pyrido[3,4-*b*]indole (**4**), which has both carbamate and amide functional groups. The selection of this molecule was based upon the unique semi-rigid conformation of the pyrazino[2′,1′:6,1]pyrido[3,4-*b*]indole nucleus (**1**) that does not acquire any dynamic behavior and also possesses CNS depressant,[7] antihistaminic,[8] hypotensive,[6] phosphodiesterase inhibitory,[9] and neoplasm inhibitory activities.[10]

The synthetic methodology commenced with the synthesis of 2-[(4-methylphenyl)sulfonyl]-1,2,3,4,6,7,12,12a(*S*)-octahydropyrazino[2′,1′:6,1]pyrido[3,4-*b*] indole (**2**) from the tosylation of the previously reported 1,2,3,4,6,7,12,12a(*S*)-octahydropyrazino[2′,1′:6,1]pyrido[3,4-*b*]indole molecule[6] (**1**) using tosyl chloride in pyridine. This was followed by the reduction of indole double bond using boranedimethylsulfide complex[11] in the presence of TFA at 0 °C. The reaction was completed in 3 h providing 2-[(4-methylphenyl)-sulfonyl]-1,2,3,4,6,6a,7,11b,12,12a(*S*)-decahydropyrazino-[2′,1′:6,1]pyrido[3,4-*b*]indole (**3**) with a high degree of purity and yield. Finally, compound **4** was prepared by the amidation of **3**, treating it with carbobenzyloxy-L-alanine in the presence of coupling agent DIC in dichloromethane. The overall yield of compound **4** achieved after three steps of reaction was 47% (Scheme 1).

Once the synthesis of the final compound (**4**) was achieved, the complete structure elucidation was carried out using various one- and two-dimensional NMR experiments. The unequivocal assignments of **4** were performed by the combined use of ^{1}H, ^{13}C, DEPT, COSY, edited HSQC, HMBC, and NOESY NMR spectra recorded in three solvents, in $CDCl_3$ at 248 K and in $(CD_3)_2CO$ and DMSO-d_6 solution at 298 K.

2.2. Exchange phenomenon in $CDCl_3$ solution

The ^{1}H NMR spectrum of **4** recorded at 298 K in $CDCl_3$ solution showed pronounced line broadening of all the resonances, revealing the expected dynamic exchange process in the system. Hindered rotation around the amide C–N bond was indicated by the signal of the H-8 proton, which appeared distinctly as a broad resonance at 7.8 ppm in ^{1}H NMR spectrum recorded in $CDCl_3$ solution at 298 K, and further emerged as an *ortho*-coupled doublet resonating at 8.0 ppm on decreasing the temperature to 248 K (Fig. 1a). The HSQC spectrum recorded at 248 K allowed observation of cross peaks owing to two rotamers and the exact ratio of population of rotamers was found to be 4:1 by taking the integral values of the partially resolved signals.

Moreover, the 2D exchange spectrum recorded at 248 K showed fully resolved exchange cross peaks for H-8 proton (Fig. 1b) further reinstating the hindered rotation of amide C–N bond of the carbobenzyloxy-L-alanyl side chain in the molecule. The rotation around the carbamate C–N bond was found beyond the NMR time-scale in $CDCl_3$ solution as no exchange cross peak for the NH proton was observed at any temperature. Armed with these observations it was stated that in $CDCl_3$ solution at 298 K, the presence of two populations was clearly visible but can only be determined within NMR time-scale by restricting the rotation around amide C–N bond at a low temperature of 248 K. The magnitude of the downfield shift of the major H-8 proton and upfield shift of minor H-8 proton also indicated the conformation of the molecule as reported earlier by Nagarajan et al. in case of *N*-acylindolines.[12] Although the exact conformation of both the rotamers was not deduced at this point of time, it was presumed that at lower temperature (248 K), the CO group is preferentially oriented toward the phenyl ring (rotamer A) while at room temperature it was in its reverse orientation (rotamer B). These presumptions were further supported by the results obtained by theoretical studies using Maestro 7.0.113 suite of programs with MMFF's force field.

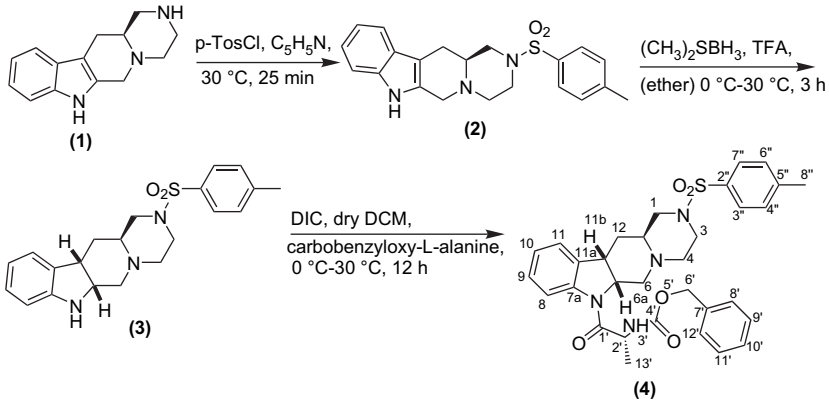

Scheme 1. Strategy for the synthesis of **4**.

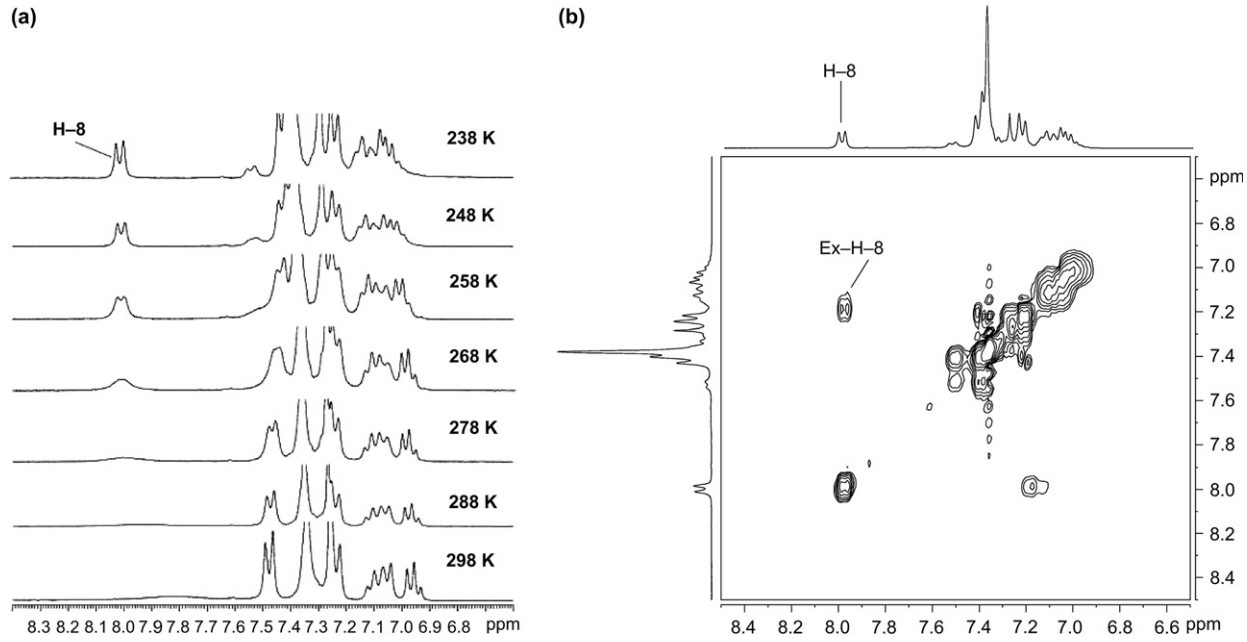

Figure 1. (a) ^{1}H NMR spectrum of **4** in $CDCl_3$ solution as a function of temperature. (b) Expanded region of NOESY spectrum showing exchange cross peak for H-8 in $CDCl_3$ solution at 248 K.

2.3. Exchange phenomenon in $(CD_3)_2CO$ and DMSO-d_6 solutions

Since the rotation around the carbamate C–N bond was not observed in $CDCl_3$ solution at any temperature, the exchange phenomenon was further re-examined in polar solvents, viz., DMSO-d_6 and $(CD_3)_2CO$. Contrary to $CDCl_3$ solution, 2D exchange spectra recorded in $(CD_3)_2CO$ and DMSO-d_6 solutions revealed the exchange cross peak for the NH proton (Fig. 2). No exchange cross peak for the H-8 proton was observed in either solvent in the temperature range of 278–318 K. These observations straightforwardly suggested the existence of slow hindered rotation of the carbamate C–N bond in $(CD_3)_2CO$ and DMSO-d_6, that is within the NMR time-scale whereas the rotation of the amide C–N bond was not observed in these solvents.

2.4. Kinetics of exchange process

To establish the kinetic order of both the exchange processes, the concentration dependence of the NOESY spectra has been studied. No variation was found in the intensity of the cross peak for the NH proton in DMSO-d_6 and the H-8 proton in $CDCl_3$ solution upon diluting the initial solution concentration to its half value at 298 K taking the mixing time of τ_m=200 ms. Under these conditions the exchange

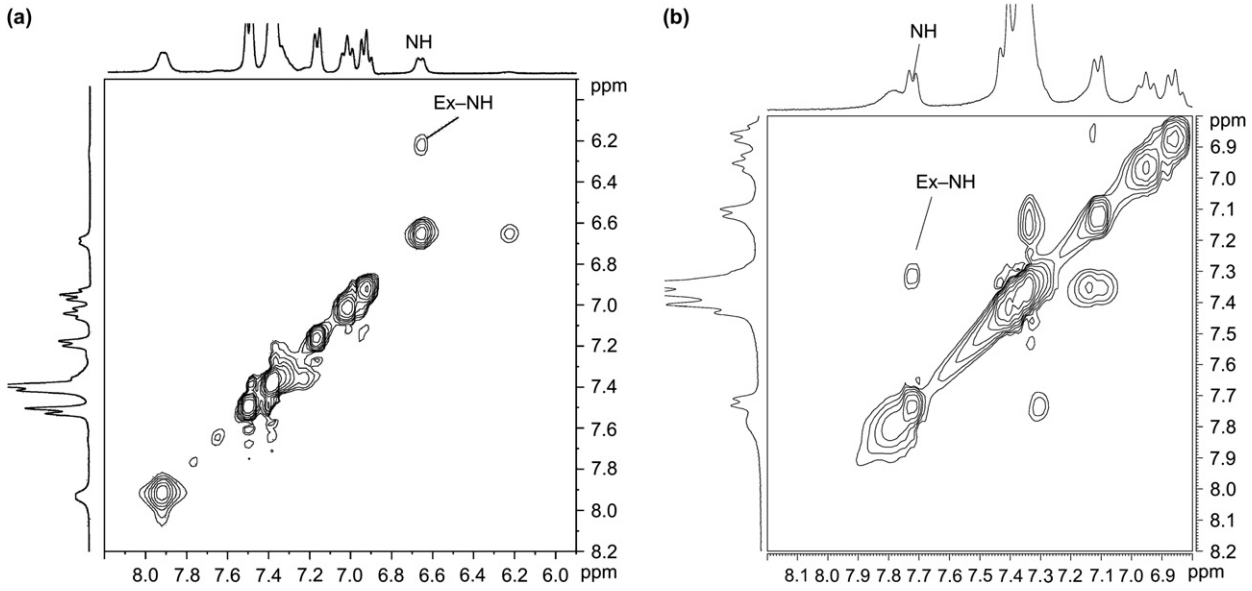

Figure 2. Expanded region of NOESY spectrum showing exchange cross peak for NH in (a) $(CD_3)_2CO$ and (b) DMSO-d_6 solutions.

was about 13% complete in DMSO-d_6 and 24% in $CDCl_3$ solution. Since any substantial change in the rate constants would immediately be reflected in the cross peak intensities, it was therefore concluded that exchange of NH proton and H-8 proton in their respective solvents obeyed first order kinetics.[13]

The Eyring analysis of **4** was performed to estimate the barrier to rotation ($\Delta G^{\ddagger}$) around carbamate and amide C–N bonds in their respective solvents. The rates of exchange process were calculated by performing phase sensitive 2D-NOESY using mixing times of 200, 300, 400 ms in $CDCl_3$, $(CD_3)_2CO$, and DMSO-d_6 solutions at five different temperatures. These temperature ranges varied for all three solvents, as temperatures at which good separation of exchange cross peaks of the respective signals was observed were selected for the analysis. For instance, in the case of $(CD_3)_2CO$ the temperature range was 298–278 K. The values of the rate constants have been obtained by Eq. 1,[14] and presented in Tables 1 and 2.

$$K \approx 1/[t_M(I_D/I_C+1)] \quad (1)$$

I_D is the intensity of diagonal peak and I_C is the intensity of cross peak in the NOESY spectrum.

The activation parameters involved in both exchange processes were determined using the Eyring equation[15] (Eq. 2) and are presented in Tables 3 and 4 and the Eyring plots are given in Figure 3.

$$\ln(k/T) = -(\Delta H^{\ddagger}/RT) + [23.76 + (\Delta S^{\ddagger}/R)] \quad (2)$$

Similar to the previously documented analysis,[4] $\Delta G^{\ddagger}$ of our complex system did not show remarkable variation with change of solvents. Despite having two concurrent hindered rotations existing in the same system, the barrier to rotation of carbamate and amide C–N bonds was found to be $\approx$16 kcal/mol, which is also supported by the theoretically calculated value. Therefore, it was concluded that the rotational barrier of carbamate C–N bond and amide C–N bond in a particular solvent is independent of other exchange processes existing in the same system.

Table 1. Rate constants determined using Eq. 1 in $(CD_3)_2CO$ and DMSO-d_6 for $\Delta G^{\ddagger}$ of carbamate bond

$(CD_3)_2CO$					
T/K	278	283	288	293	298
k_1 (s^{-1})	0.21±0.02	0.25±0.03	0.29±0.05	0.32±0.06	0.39±0.07
k_{-1} (s^{-1})	2.36±0.23	2.65±0.44	2.95±0.44	3.08±0.55	3.48±0.68
DMSO-d_6					
T/K	298	303	308	313	318
k_1 (s^{-1})	0.29±0.04	0.33±0.05	0.38±0.07	0.44±0.12	0.49±0.13
k_{-1} (s^{-1})	1.28±0.30	1.53±0.40	1.79±0.47	2.02±0.60	2.43±0.75

Table 2. Rate constants determined using Eq. 1 in $CDCl_3$ solution for $\Delta G^{\ddagger}$ of amide bond

$CDCl_3$					
T/K	238	243	248	253	258
k_1 (s^{-1})	0.22±0.02	0.31±0.04	0.41±0.04	0.54±0.04	0.72±0.07
k_{-1} (s^{-1})	0.11±0.01	0.15±0.01	0.20±0.01	0.29±0.01	0.34±0.01

Table 3. Activation parameters[a] of carbamate C–N bond obtained using Eq. 2 in $(CD_3)_2CO$ and DMSO-d_6

Solvent	$\Delta H^{\ddagger}$[b]	$\Delta S^{\ddagger}$[c]	$\Delta G^{\ddagger}$[b]
$(CD_3)_2CO$	2.89±0.98	−47.82±3.11	15.93±0.17
DMSO-d_6	4.27±1.01	−45.16±3.68	16.60±0.06

[a] 0 °C.
[b] Values in kcal/mol.
[c] Values in cal/mol.

Table 4. Activation parameters[a] of amide C–N bond obtained using Eq. 2 in $CDCl_3$

Solvent	$\Delta H^{\ddagger}$[b]	$\Delta S^{\ddagger}$[c]	$\Delta G^{\ddagger}$[b]
$CDCl_3$	6.42±0.07	−34.75±1.04	15.86±0.26

[a] 0 °C.
[b] Values in kcal/mol.
[c] Values in cal/mol.

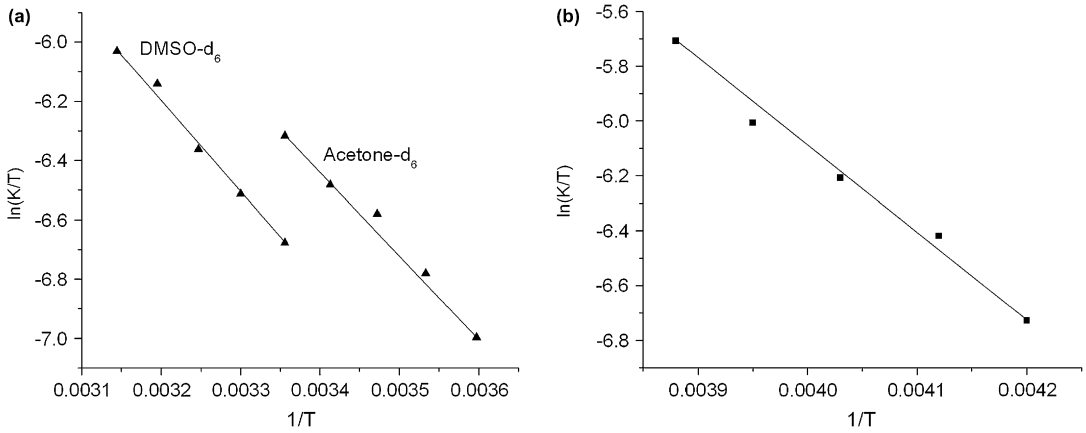

Figure 3. Eyring plots of the rate constants (a) in $(CD_3)_2CO$ and DMSO-d_6, (b) in $CDCl_3$ solution with 200 ms mixing time determined by fitting the rate constants to the experimental data at five different temperatures.

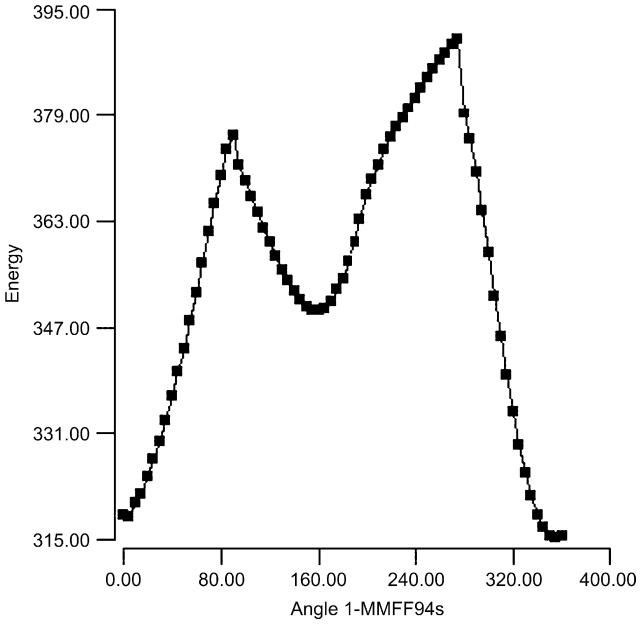

Figure 4. Conformational profile for **4** obtained for amide C–N bond rotation at the molecular mechanics (MMFF) level of theory.

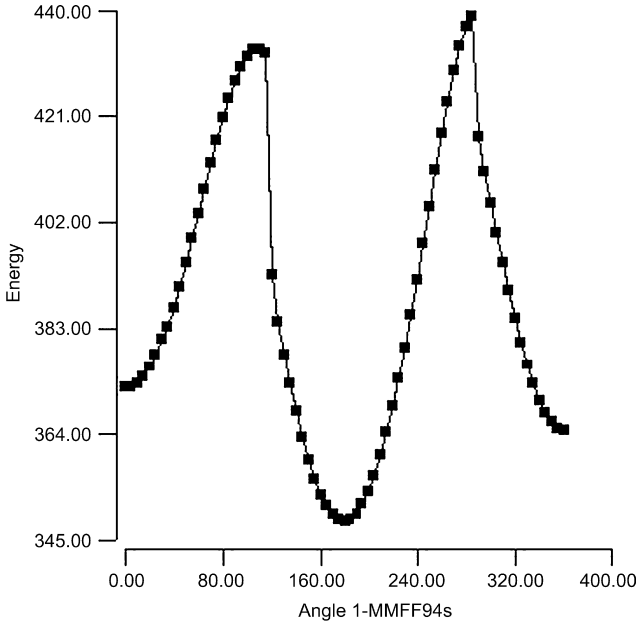

Figure 6. Conformational profile for **4** obtained for carbamate C–N bond rotation at the molecular mechanics (MMFF) level of theory.

2.5. Theoretical studies

What is immediately striking from our observations is that free rotation along the C–N bond can cause a difference in the magnetic environment around the H-8 phenyl core and hence two signals in the NMR spectrum for H-8 proton can be observed. To gain insight into the problem of how the amide group at indole-N may be impacting the variation in the magnetic field of H-8 proton via changes in the conformation and also to obtain the exact conformation of these two rotamers along with the confirmation of the barrier to rotation of the four rotamers, conformational dynamics of **4** was studied. The minimum energy conformation of **4** was obtained using Maestro 7.0.113 suite of programs with MMFF's force field. The energy minimized conformation (total energy 315.4 kJ/mol) shows that the structure adopts a conformation where the carbonyl group is facing the phenyl ring (rotamer A). In order to visualize the effect of rotation along C–N bond on the overall energy (potential energy) of the molecule, a conformational search (Fig. 4) was carried out employing macromodel module, dihedral drive with an increment of 5° rotation over 360°. Inspection of the results reveals that the dip in Figure 4 corresponds to rotamer B (349.6 kJ/mol) having undergone a rotation of ~160° from the initial structure. The carbonyl group in rotamer B lies almost opposite to the phenyl ring as predicted earlier by NMR study. The above results clearly indicate the appearance of two NMR signals for H-8 proton (Fig. 5). The $\Delta G^{\ddagger}$ values for **4**, obtained from Figure 4, show that rotamers A and B can be inter-converted

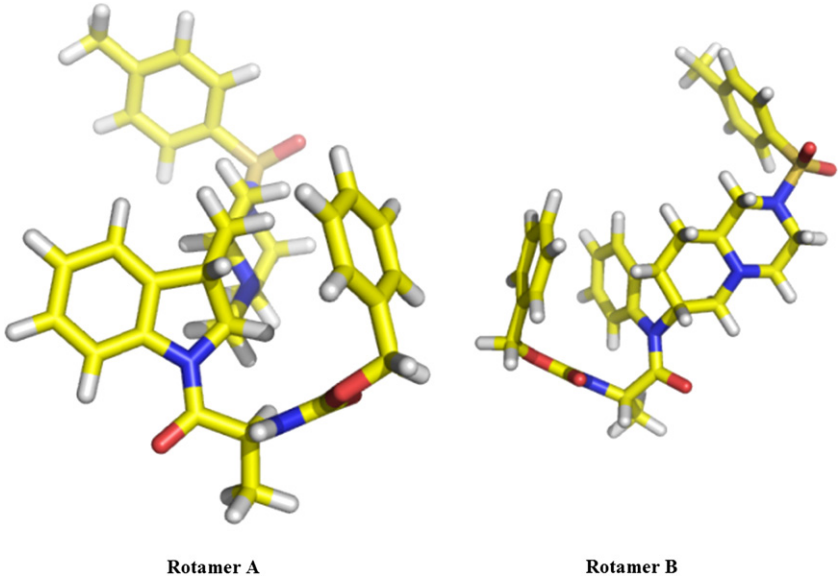

Figure 5. Exact conformation of the two rotamers A and B obtained in $CDCl_3$ due to amide C–N bond rotation.

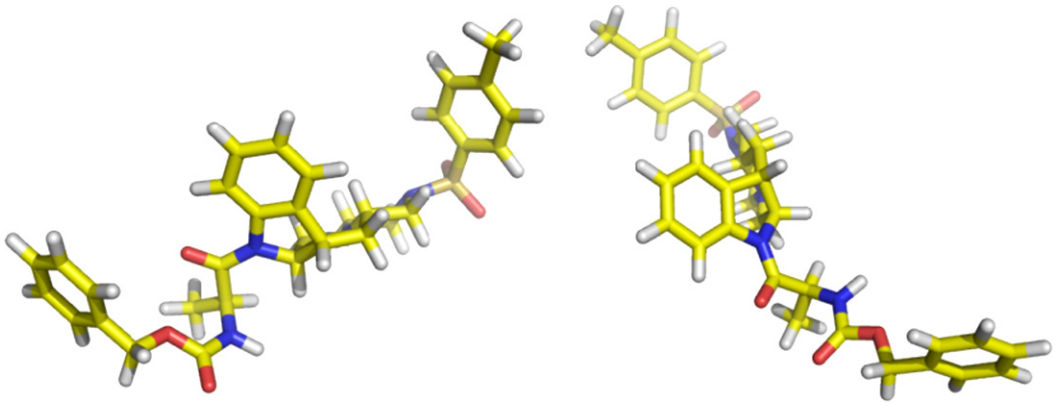

Rotamer C Rotamer D

Figure 7. Exact conformation of the two rotamers C and D obtained in DMSO-d_6 due to carbamate C–N bond rotation.

by overcoming energy barriers of 14.46 kcal/mol (60.46 kJ/mol).

Similar conformational dynamics study of the molecule **4** was carried out for the identification of the two rotamers, which originated due to restricted rotation along the carbamate C–N bond. Since the restricted rotation of the carbamate C–N bond was observed in the case of DMSO-d_6 and $(CD_3)_2CO$ and not in $CDCl_3$, the exact conformation for the molecule **4** in DMSO-d_6 was calculated using MMFF's force field. The molecular modeling was carried out using water as a solvent and keeping the dielectric constant of DMSO at 298 K. The energy minimized conformation (total energy 364.79 kJ/mol) shows that the structure adopts a conformation where the carbonyl group of the carbamate is parallel to the NH (rotamer C). Examination of results again reveals that the dip in Figure 6 corresponds to rotamer D (383.53 kJ/mol) having incorporated rotation of ~170° from the initial structure. The carbonyl group in rotamer B lies almost opposite to the NH group in this case. The $\Delta G^{\ddagger}$ values for **4**, obtained in DMSO-d_6 from Figure 6, indicated that rotamers C and D can be interconverted by overcoming energy barriers of 16.41 kcal/mol (68.63 kJ/mol) (Fig. 7).

2.6. Biological activity

In vitro receptor binding studies for dopaminergic (D_2) and seratonergic (5-HT_{2A}) were carried out using rat brain caudate region and cortex membrane, respectively. The radioligand and reference compound used for D_2 receptor binding studies were [^{3}H] Spiperone and Haloperidol (K_i=0.43 nM), respectively, and for 5-HT_{2A} receptor binding studies the radioligand and reference compound used were [^{3}H] Ketanserin and Ketanserin (K_i=0.38 nM), respectively. Compound **4** has shown a very good affinity for 5-HT_{2A} receptors (K_i=0.52 nM) with no affinity for the D_2 receptor. The selectivity of this compound toward seratonergic receptors may be converted into its use as an antidepressant. The compound has also shown 16% antihistaminic (H_1) activity (at 1 μg/mL) when tested on Guinea pig ileum (GPI) for blockade of histamine-induced contractions. The standard drug used in this case was Ceterizine with 34% histamine blockade (at 1 μg/mL).

3. Conclusions

In summary, our investigations demonstrated the complex dynamic behavior of (6a*R**,11b*S**)-7-[carbobenzyloxy-L-alanyl]-2-[(4-methylphenyl)sulfonyl]-1,2,3,4,6,6a,7,11b,12,12a(*S*)-decahydropyrazino[2′,1′:6,1]pyrido[3,4-*b*]indole (**4**). The molecule was specifically synthesized for the first time to examine the mutual effect of the hindered rotation around carbamate and amide C–N bonds and it demonstrated the presence of four rotamers of the molecule. It was proposed using concentration dependent NOESY experiment that both the exchange processes obey first order kinetics. The barrier to rotation of both amide and carbamate bonds of **4** was found to be around 15–16 kcal/mol by both dynamic NMR calculations and theoretical calculations and typically insensitive to the coexisting bond rotations. Our study signifies a new dimension to the ongoing research in this field to explore such type of complex systems bearing two or more functional groups. Moreover, the molecule has been found to be active as antidepressant, it is therefore believed that the effect of this dynamic behavior using similar types of substitutions may be one of the deciding factors in influencing the activity profile of these classes of compounds.

4. Experimental

4.1. General considerations

All the solvents used for the reactions and purifications were commercially available and used after distillation. All the products were characterized by ^{1}H, ^{13}C, DEPT90, DEPT135, two-dimensional Correlation Spectroscopy (COSY), Heteronuclear Single Quantum Coherence (HSQC), and Heteronuclear Multiple Bond Correlation spectroscopy (HMBC).

The NMR spectra were recorded using a BRUKER Avance DRX 300 MHz FT NMR spectrometer equipped with a 5 mm multinuclear inverse probehead with z-shielded gradient. Experiments were recorded in DMSO-d_6, $(CD_3)_2CO$, and in $CDCl_3$ in the temperature range from 298 K to 248 K. Chemical shifts are given on the δ scale and are referenced to TMS at 0.00 ppm for the proton and 0.00 ppm for the carbon. In the 1D measurement (^{1}H and ^{13}C) 32K data points

were used for the FID. The pulse programs of the following 2D experiments were taken from the Bruker software library and the parameters were as follows.

300/75 MHz gradient HSQC spectra: relaxation delay d1=2 s; evolution delay d2=3.44 ms; 90° pulse, 6.85 μs for ^{1}H, 10 μs for ^{13}C, hard pulses at −3.0 dB and 60 μs for ^{13}C GARP decoupling with gradient ratio GPZ1:GPZ2: GPZ3=50:30:40.1; 1024 data points in t2; spectral width 9.0 ppm in F2 and 160 ppm in F1; number of scans 32; 256 experiments in t1; linear prediction to 512; zero filling up to 1K and apodization with sine-bell in both dimensions prior to double Fourier transformation.

300/75 MHz gradient HMBC spectra: relaxation delay d1=2 s; delay of the low-pass *J*-filter d2=3.44 ms; delay for evolution of long-range coupling d6=71 ms with gradient ratio same as HSQC; 2048 data points in t2; spectral width 11.0 ppm in F2 and 240 ppm in F1; number of scans 52; 256 experiments in t1; linear prediction to 512; zero filling up to 2K and apodization with 90° shifted square sine-bell in F1 dimension and sine-bell in F2 dimension prior to double Fourier transformation.

4.1.1. General procedure for the synthesis of 1,2,3,4,6,7,12,12a(*S*)-octahydropyrazino[2′,1′:6,1]pyrido[3,4-*b*]indole (1). Compound **1** was prepared by reported procedure taking (*S*)-(−)-tryptophan as starting material.[6] ^{1}H NMR (300 MHz, DMSO-d_6) 298 K, δ=3.07 (m, 3H, H-12a, H-12ax, H-4ax), 3.27 (t(o), 1H, H-1ax), 3.37 (m, 1H, H-12eq), 3.50 (t(o), 1H, H-3eq), 3.61 (t(o), 2H, H-3ax, H-4eq), 3.76 (d, *J*=11.8 Hz, 1H, H-1eq), 4.06 (d, *J*=15.2 Hz, 1H, H-6ax), 4.35 (t(o), 1H, NH-2), 4.56 (d, *J*=14.9 Hz, 1H, H-6eq), 7.70 (t(o), 1H, H-10), 7.78 (t(o), 1H, H-9), 8.05 (d(o), *J*=8.0 Hz, 1H, H-11), 8.10 (d(o), *J*=7.7 Hz, 1H, H-8), 11.52 (s, 1H, NH-7); ^{13}C NMR (75 MHz, DMSO-d_6) 298 K, δ=25.6 (C-12), 45.7 (C-3), 52.1 (C-6), 52.4 (C-1), 55.9 (C-4), 57.9 (C-12a), 105.5 (C-11b), 110.5 (C-11), 117.3 (C-8), 118.3 (C-10), 120.3 (C-9), 126.6 (C-11a), 131.9 (C-6a), 135.8 (C-7a). Mass (FAB) *m*/*z* 228 (M^{+}+1). Anal. Calcd for $C_{14}H_{17}N_3$: C, 73.98; H, 7.54; N, 18.49. Found C, 74.05; H, 7.56; N, 18.59.

4.1.2. 2-[(4-Methylphenyl)sulfonyl]-1,2,3,4,6,7,12,12a(*S*)-octahydropyrazino[2′,1′:6,1]pyrido[3,4-*b*]indole (2). A solution of **1** (1.4 g, 6.0 mmol) and 4-toluenesulfonyl chloride (1.4 g, 7.2 mmol) in dry pyridine 15 mL was stirred at 30 °C for 25 min. The solid separated was filtered off, washed with water (6×50 mL), and crystallized from C_2H_5OH/H_2O to give light yellow crystals of **2** (1.53 g, 65%) mp 178 °C. IR (KBr): $\tilde{\nu}$ 3361, 2904, 2833, 2364, 1592, 1450, 1360, 1164, 742, 658, 547 cm^{-1}. FABMS: *m*/*z* 382 [M+H^{+}]. ^{1}H NMR (300 MHz, $CDCl_3$) 298 K, δ=2.36 (m, 1H, H-4ax), 2.44 (s, 3H, H-8′), 2.55 (m, 1H, H-12ax), 2.64 (m, 2H, H-3eq, H-6ax), 2.75 (s, 1H, H-12a), 2.83 (m, 1H, H-12eq), 3.04 (m, 1H, H-6eq), 3.54 (d, *J*=14.3 Hz, 1H, H-1ax), 3.64 (br s, 1H, H-3ax), 3.78 (d, *J*=10.9 Hz, 1H, H-1eq), 3.88 (d, *J*=14.3 Hz, 1H, H-4eq), 7.10 (m, 2H, H-9, H-10), 7.28 (d, *J*=7.7 Hz, 1H, H-8), 7.34 (d, *J*=8.1 Hz, 2H, H-4′, H-6′), 7.41 (d, *J*=7.5 Hz, 1H, H-11), 7.68 (d (o), *J*=8.1 Hz, 2H, H-3′, H-7′); ^{13}C NMR (75 MHz, $CDCl_3$) 298 K, δ=21.8 (C-8′), 25.5 (C-12), 46.3 (C-3), 51.6 (C-1), 51.8 (C-4), 53.8 (C-6), 56.3 (C-12a), 106.7 (C-11b), 110.9 (C-8), 118.1 (C-11), 119.8 (C-10), 121.9 (C-9), 127.1 (C-11a), 128.1 (C-3′, 7′), 129.4 (C-4′, 7′), 130.3 (C-2′), 132.4 (C-6a), 136.2 (C-7a), 144.1 (C-5′). Mass (FAB) *m*/*z* 382 (M^{+}+1). Anal. Calcd for $C_{21}H_{23}N_3O_2S$: C, 66.12; H, 6.08; N, 11.01. Found C, 66.05; H, 6.15; N, 11.02.

4.1.3. (6a*R,11b*S**)-2-[(4-Methylphenyl)sulfonyl]-1,2,3,4,6,6a,7,11b,12,12a(*S*)-decahydropyrazino[2′,1′:6,1]-pyrido[3,4-*b*]indole (3).** A solution of borane dimethyl sulfide complex (10 M, 0.5 mL) was added dropwise to a stirred solution of **2** (0.95 g, 2.5 mmol) in trifluoroacetic acid (7.3 mL) at 0 °C in an atmosphere of nitrogen for 10 min. The reaction mixture was stirred for another 3 h at 30 °C. Workup was done by adding water (0.5 mL) to the reaction mixture, concentrating, and basifying with ammonia solution. The precipitated product was filtered off and crystallized from ethanol/water to give white crystals of **3** (0.65 g, 68%), mp 110 °C. IR (KBr): $\tilde{\nu}$ 3367, 2922, 2834, 1596, 1350, 1165, 1005, 760, 742, 658, 550 cm^{-1}. FABMS: *m*/*z* 384 [MH^{+}]. ^{1}H NMR (300 MHz, $CDCl_3$) 298 K, δ=1.07 (m, 1H, H-12ax), 1.68 (m, 1H, H-12eq), 1.96 (t, *J*=10.4 Hz, 1H, H-1ax), 2.11 (m, 1H, H-12a), 2.34 (m, 1H, H-4ax), 2.38 (s, 3H, H-8′), 2.43 (m, 1H, H-6ax), 2.53 (dt, *J*=2.3 Hz and 11.5 Hz, 1H, H-3eq), 2.83 (br d, *J*=11.3 Hz, 1H, H-4eq), 2.99 (m, 1H, H-11b), 3.11 (d, *J*=13.5 Hz, 1H, H-6eq), 3.50 (m, 1H, H-1eq), 3.63 (dd, *J*=1.8 Hz and 10.5 Hz, 1H, H-3ax), 3.81 (br d, *J*=6.1 Hz, 1H, 6a), 6.64 (d, *J*=7.8 Hz, 1H, H-8), 6.71 (dt, *J*=0.5 Hz and 7.5 Hz, 1H, H-10), 6.97 (dt, *J*=1.0 Hz and 7.6 Hz,1H, H-9), 7.08 (d, *J*=7.2 Hz, 1H, H-11), 7.26 (d, *J*=8.1 Hz, 2H, H-3′ and H-7′), 7.57 (d, *J*=8.1 Hz, 2H, H-4′ and H-6′); ^{13}C NMR (75 MHz, $CDCl_3$) 298 K, δ=21.6 (C-13′), 33.8 (C-12), 38.6 (C-11b), 45.9 (C-3), 51.3 (C-1), 54.2 (C-4), 56.2 (C-6), 57.1 (C-12a), 58.9 (C-6a), 111.0 (C-8), 119.5 (C-10), 123.6 (C-11), 127.8 (C-9), 128.1 (C-3′, 7′), 129.7 (C-4′, 7′), 131.9 (C-2′), 134.5 (11b), 143.9 (C-5′), 150.1 (C-7a). Mass (FAB) *m*/*z* 384 (M^{+}+1). Anal. Calcd for $C_{21}H_{25}N_3O_2S$: C, 65.77; H, 6.57; N, 10.96. Found C, 65.75; H, 6.59; N, 11.02.

4.1.4. (6a*R,11b*S**)-7-[Carbobenzyloxy-L-alanyl]-2-[(4-methylphenyl)sulfonyl]-1,2,3,4,6,6a,7,11b,12,12a(*S*)-decahydropyrazino[2′,1′:6,1]pyrido[3,4-*b*]indole (4).** DIC (0.2 mL, 1.3 mmol) was added to a stirred solution of carbobenzyloxy-L-alanine (0.3 g, 1.3 mmol) in dry DCM (15 mL), stirring was continued for another 20 min and this reaction mixture was cooled to 0 °C. Compound **3** (0.5 g, 1.3 mmol) was added to the above mixture in portions at 0 °C during 15 min. The reaction mixture was stirred for another 12 h at 30 °C. The reaction mixture was filtered and the filtrate was concentrated under vacuum, water was added to the residue, and extracted with ethyl acetate (3×30 mL). The combined ethyl acetate layer was washed with water, dried over sodium sulfate, and concentrated to one third of the volume. The separated diisopropyl urea was filtered off and the filtrate was finally concentrated. The residue obtained was subjected to crystallization using methanol yielding white needle-like crystals of **4** (0.52 g, 67.5%); mp 190° C. IR (KBr): $\tilde{\nu}$ 3383, 2829, 2363, 1712, 1658, 1597, 1362, 1238, 1162, 1114, 1024, 757 cm^{-1}. FABMS: *m*/*z* 589 [M+H^{+}]. ^{1}H NMR (300 MHz, $CDCl_3$) 298 K, δ=1.26 (br s, 2H, H-12), 1.38, (d, *J*=6.3 Hz, 3H, H-13′), 1.89 (t, *J*=10.2 Hz, 1H, H-1ax), 2.10 (m, 1H,

H-3eq), 2.41 (s, 3H, H-8″), 2.54 (m, 1H, H-12a), 2.63 (m, 3H, H-6, H-4ax), 3.04 (s, 1H, H-4eq), 3.35 (br d, 2H, H-1eq, H-3ax), 3.51 (s, 1H, H-11b), 4.44 (br s, 1H, H-6a), 4.68 (br s, 1H, H-2′), 5.09 (q, J=9.2 Hz, 2H, H-6′), 5.65 (br s, 1H, NH), 6.94 (t, J=6.9 Hz, 1H, H-10), 7.04 (m, 2H, H-11, H-9), 7.23 (d, J=7.6 Hz, 2H, H-4″, 6″), 7.33 (s, 5H, H-8′, H-9′, H-10′, H-11′, H-12′), 7.48 (d, J=7.4 Hz, 2H, H-3″, H-7″), 7.79 (br s, 1H, H-8); ^{13}C NMR (75 MHz, $CDCl_3$) 298 K, δ=19.8 (C-13′), 21.7 (C-8′), 29.9 (C-12), 37.3 (C-11b), 44.6 (C-3), 49.5 (C-2′), 49.7 (C-1), 52.8 (C-4), 53.2 (C-6), 56.5 (C-12a), 60.0 (C-6a), 67.1 (C-6′), 116.8 (C-8), 123.2 (C-11), 124.1 (C-10), 127.6 (C-9), 127.8 (C-3″, 7″), 128.1 (C-10′), 128.3 (C-8′, 12′), 128.7 (C-9′, 11′), 129.7 (C-4″, 6″), 132.7 (C-2″), 134.7 (C-11a), 136.5 (C-7′), 142.7 (C-7a), 143.7 (C-5″), 155.9 (C-4′), 171.8 (C-1′). Mass (FAB) m/z 589 (M^++1). Anal. Calcd for $C_{32}H_{36}N_4O_5S$: C, 65.28; H, 6.16; N, 9.52. Found C, 65.25; H, 6.19; N, 9.55.

4.2. Standard protocols used for determining biological activities

4.2.1. Dopamine (D_2) receptor binding. Brains were isolated by decapitation of Sprague Dawley rats of either sex with 200–250 g body weight. Caudate regions of the brain were dissected out at 4 °C. Immediately tissues were homogenized in 50 mM Tris buffer of pH 7.7. The homogenates were centrifuged at 50,000×g at 4 °C. Pellets obtained were washed twice in the above buffer followed by resuspending in Tris-salt buffer. Tissue suspension was incubated at 37 °C for 10 min followed by centrifugation at 50,000×g at 4 °C. Final tissue pellets were resuspended in Tris-salt buffer, aliquoted, and stored at −20 °C until binding assays. Ligand binding assays were carried out by incubating 300 μg membrane protein suspension with various concentrations of test drug at 37 °C for 20 min in 1 mL incubation mixture containing 50 mM ketanserin, 0.067 nM [^{3}H]-spiperone. After completion of the incubation, the reaction was terminated by filtering the incubation mixture using Whatman GF/C filters under vacuum. Dried filters were collected and placed in scintillation vials to which was added 5 mL of scintillation cocktail. Non-specific binding was determined using similar conditions in the presence of 100 nM haloperidol. Scintillation counts were determined and data were analyzed by non-linear regression analysis to determine K_i and IC_{50} of test drug using Graph pad Prism software.

4.2.2. Serotonin 5-HT_{2A} binding. Potency of test compounds to bind to serotonin 5-HT_{2A} receptors was determined using cortex membranes prepared by isolating brain from Sprague Dawley rats of either sex of 200–250 g body weight. Cortex regions were dissected out and homogenized in 50 mM Tris buffer, pH 7.7. Pellets were washed twice and resuspended in the same buffer. Competitive binding assays were carried out by incubating 300 μg protein with 0.39 nM [^{3}H]-ketanserin at 37 °C for 20 min in the presence of various concentrations of test drug to a final volume of 1 mL. Incubation mixtures were filtered onto Whatman GF/C filters. Filters were collected followed by addition of scintillation cocktail. Scintillation counts were obtained and data were analyzed by non-linear regression analysis to determine K_i and IC_{50} using Graph pad Prism software.

Acknowledgements

A.A., A.D.R., and R.C. are thankful to CSIR New Delhi for providing fellowship. The authors are extremely grateful to Dr. Rajesh K. Grover of The Scripps Research Institute, La Jolla, California for his valuable suggestions and theoretical MMFF calculations.

Supplementary data

Supplementary data associated with this article can be found in the online version, at doi:10.1016/j.tet.2007.03.171.

References and notes

1. Stewart, W. E.; Siddall, T. H., III. *Chem. Rev.* **1970**, *70*, 517–551.
2. (a) Rablen, P. R. *J. Org. Chem.* **2000**, *65*, 7930–7937; (b) Suarez-Castillo, O. R.; Contreras-Martinez, Y. M. A.; Beiza-Granados, L.; Melendez-Rodriguez, M.; Villagomez-Ibarra, J. R.; Torres-Valencia, J. M.; Morales-Rios, M. S.; Joseph-Nathan, P. *Tetrahedron* **2005**, *61*, 8809–8820; (c) Kam, T. S.; Yoganathan, K.; Li, H.-Y. *Tetrahedron Lett.* **1996**, *37*, 8811–8814.
3. Scherer, G.; Kramer, M. L.; Schutkowski, M.; Reimer, U.; Fischer, G. *J. Am. Chem. Soc.* **1998**, *120*, 5568–5574.
4. Lectka, T.; Cox, C. *J. Org. Chem.* **1998**, *63*, 2426–2427.
5. Deetz, M. J.; Forbes, C. C.; Jonas, M.; Malerich, J. P.; Smith, B. D.; Wiest, O. *J. Org. Chem.* **2002**, *67*, 3949–3952.
6. Saxena, A. K.; Jain, P. C.; Anand, N.; Dua, P. R. *J. Med. Chem.* **1973**, *16*, 560–564.
7. (a) Kumar, N.; Dhoan, M. K.; Agarwal, S. K.; Saxena, A. K.; Jain, P. C.; Anand, N. *Eur. J. Med. Chem.* **1982**, *17*, 312–316; (b) Kumar, N.; Dhoan, M. K.; Agarwal, S. K.; Saxena, A. K.; Jain, P. C.; Anand, N. *Indian J. Chem.* **1980**, *19b*, 1087–1088.
8. (a) Saxena, A. K.; Dhoan, M. K.; Ram, S.; Saxena, M.; Jain, P. C.; Patnaik, G. K.; Anand, N. *Indian J. Chem.* **1983**, *22b*, 1224–1232; (b) Saxena, M.; Agarwal, S. K.; Patnaik, G. K.; Saxena, A. K. *J. Med. Chem.* **1990**, *33*, 2970–2976.
9. (a) Jiang, W.; Alford, V. C.; Qiu, Y.; Bhattacharjee, S.; Mathew, T. J.; Haynes-Jhonson, D.; Kraft, P. J.; Lundeen, S. G.; Sui, Z. *Bioorg. Med. Chem.* **2004**, *12*, 1505–1515; (b) Daugan, A.; Grondin, P.; Ruault, C.; Le Monnier de Gouville, A.-C.; Coste, H.; Kirilovsky, J.; Hyafil, F.; Labaudiniere, R. *J. Med. Chem.* **2003**, *46*, 4525–4532; (c) Daugan, A.; Grondin, P.; Ruault, C.; Le Monnier de Gouville, A.-C.; Coste, H.; Kirilovsky, J.; Hyafil, F.; Labaudiniere, R. *J. Med. Chem.* **2003**, *46*, 4533–4542.
10. Pamukcu, R.; Larry, A. P. U.S. Patent 6,046,199, April 4, 2000; *Chem. Abstr.* **2000**, *132*, 257762.
11. Rao, J.; Chakrabarty, R.; Roy, R.; Mishra, A.; Saxena, A. K. *Arkivoc* **2005**, *ii*, 20–28.
12. (a) Nagrajan, K.; Nair, M. D.; Pillai, P. M. *Tetrahedron* **1967**, *23*, 1683–1690; (b) Anderson, J. E.; Lehn, J. M. *Tetrahedron* **1968**, *24*, 123–125.
13. Grover, R. K.; Maurya, R.; Roy, R. *Tetrahedron* **2004**, *60*, 2005–2010.
14. Ernst, R. R.; Bodenhausen, G.; Wokaun, A. *Principle of Magnetic Resonance in One and Two Dimensions*; Clerendon: Oxford, 1987; p 499.
15. Günther, H. *NMR Spectroscopy Basic Principles, Concepts, and Applications in Chemistry*; Wiley: New York, NY, 1995; p 342.